Available online at www.sciencedirect.com
ScienceDirect
Materials Research Bulletin 43 (2008) 3382–3388
Materials Research Bulletin
www.elsevier.com/locate/matresbu

Inorganic phosphate crystal $Na_{15-n}[Al(PO_4)_2F_2]_{3-n}[Ti(PO_4)_2F_2]_n$ $(0 \leq n < 1)$: A novel cation exchanger with high exchange selectivity for Li^+ and Pb^{2+} ions

Ying Zhang, Peng Tian, Shigang Zhang, Yinfeng Zhao, Guangyu Liu, Yingli Wang, Zhongmin Liu *

Applied Catalysis Laboratory, Dalian Institute of Chemical Physics, Chinese Academy of Sciences, 457 Zhongshan Road, Dalian 116023, China

Received 27 November 2007; received in revised form 14 January 2008; accepted 8 February 2008
Available online 15 February 2008

Abstract

A series of inorganic phosphate crystals have been hydrothermally synthesized, which have high chemical stability and can keep their crystal structure after acid/base treatments. Its cation-exchange properties have been investigated and the results show that it is an excellent ion exchanger with high exchange capacities for H^+, Li^+ and Pb^{2+} ions (12.74, 6.98 and 3.92 mequiv./g, respectively). Selective extractions of Li^+ and Pb^{2+} from the synthetic mixtures containing (Li^+, Sr^+, K^+, Mg^{2+}, Ca^{2+} and Ba^{2+}) and (Pb^{2+}, Ca^{2+}, Ba^{2+}, Co^{2+}, Ni^{2+}, Zn^{2+} and Mg^{2+}) have been observed. The reasons of the high exchange selection of NATP for Li^+ and Pb^{2+} ions have been discussed.

Keywords: A. Inorganic compounds; C. X-ray diffraction; D. Crystal structure; D. Thermodynamic properties

1. Introduction

Since the classical work of Amphlet [1] and Clearfield et al. [2], numerous inorganic ion exchangers have been synthesized and their properties have been studied. Advancement in inorganic ion exchangers is not only due to their high thermal stability and resistivity but also for their unusual selectivity for ionic species and versatility in separation sciences. Efforts for new selective ion exchangers have been undertaken in last few decades, among which Pb^{2+} ion-selective exchangers [3–7] and Li^+ ion-selective exchangers [8–10] have attracted attention for their applications in wastewater treatment and lithium extraction.

In our previous work [11], we have reported the synthesis and structure of a novel inorganic solid electrolyte $Na_{14.5}[Al(PO_4)_2F_2]_{2.5}[Ti(PO_4)_2F_2]_{0.5}$ (NATP), which contains a large number of Na^+ cations with high mobility in the interlamellar space and the cavities of its layered crystal framework. In this paper, we successfully extend NATP into series materials NATP-*n* ($Na_{15-n}[Al(PO_4)_2F_2]_{3-n}[Ti(PO_4)_2F_2]_n$, $0 \leq n < 1$), which have the same crystal framework structure with NATP. Its cation-exchange properties have been investigated and the results show that it is an excellent

* Corresponding author. Tel.: +86 411 84685510; fax: +86 411 84691570.
E-mail address: liuzm@dicp.ac.cn (Z. Liu).

0025-5408/$ – see front matter © 2008 Elsevier Ltd. All rights reserved.
doi:10.1016/j.materresbull.2008.02.006

Table 1
Synthesis and properties of NATP-*n*

Sample code	Condition of synthesis (molar ratio)					Concentration of Al and Ti by XRF (using oxides list)	
	Ti	Al	P	F	H_2O	Al_2O_3 (wt%)	TiO_2 (wt%)
NATP-0	0	40	160	40	400	16.45	0
NATP-0.4	5	35	160	40	400	10.06	2.59
NATP-0.5 (NATP)	10	30	160	40	400	11.18	3.36
NATP-0.6	15	25	160	40	400	16.68	6.88
NATP-0.8	20	20	160	40	400	9.141	4.939

ion exchanger and a promising extractant for lead and lithium. The exchange capacities of NATP for H^+, Li^+ and Pb^{2+} ions are higher than most inorganic ion exchangers and ion-exchange resins [12–17].

2. Experimental

Titanium(IV) sulfate was chemically pure and all other reagents used were of analytical reagent grade without further purifications.

2.1. Synthesis

Samples of NATP-*n* were synthesized from mixtures of titanium(IV) sulfate, aluminum nitrate, phosphoric acid (85 wt%), hydrofluoric acid (40 wt%) and water with varying mixing ratios as indicated in Table 1. The pH values were adjusted to 8.5 by adding the saturated NaOH solution. The mixtures were then transferred into stainless-steel autoclaves (75 ml), heated to 180 °C and kept for 7 days at this temperature. The resulting white crystals were washed several times with distilled water and dried at 100 °C for 10 h. The sample NATP-0.5 with the highest relative crystallinity was chosen for detailed studies.

2.2. Characterization and analysis

Scanning electron microscope image was obtained with a JSM-5600 operating at 10 kV. The powder X-ray diffraction patterns were recorded on a D/MAX-b X-ray diffractometer with Cu Kα radiation (λ = 1.5206 Å) with a graphite monochromator. Elemental analyses were conducted on Magix 2424 X-ray fluorescent analysis diffractometer and inductively coupled plasma-atomic emission spectrometry (ICP-AES) (TJA, Iris Advantage). The pH values of solutions were detected by pH/mV/°C Meter with automatic buffer recognition from Hanna instruments.

Chemical stability of NATP-0.5 was studied by placing samples in water and solutions of 1 M sodium hydroxide, 1 M and 10^{-3} M nitric acid, respectively. Ten grams sample was mixed with 800 ml of desired solution stirring at room temperature for 24 h. The resulting solids were filtrated off and washed three times with deionized water.

2.3. Ion-exchange and selective extraction

The ion-exchange capacities for H^+, Li^+, Ni^{2+}, Mg^{2+}, Zn^{2+}, Co^{2+}, Mn^{2+}, Ca^{2+}, Pb^{2+} and Ba^{2+} were investigated. One gram NATP-0.5 was placed in 250 ml of each solution containing an above cation. The concentration of H^+ was 0.1 M and the concentrations of other metal ions were 0.5 M. Selective extractions of Li^+ and Pb^{2+} from the synthetic mixtures containing (Li^+, Sr^+, K^+, Mg^{2+}, Ca^{2+} and Ba^{2+}) and (Pb^{2+}, Ca^{2+}, Ba^{2+}, Co^{2+}, Ni^{2+}, Zn^{2+} and Mg^{2+}) were performed on NATP-0.5. One-gram sample was treated with 250 ml of each mixture. The concentration of each metal ion in both solutions was 0.2 M.

2.4. Distribution calculation

The ability of NATP to remove an ion from the solution is expressed using the ion-exchange distribution coefficient K_d. K_d is the ratio of ion concentrations in two immiscible phases (the solid phase ion-exchange materials and the

solutions) at equilibrium. It determines the affinity of a sorbent material for a specific ion and it is calculated using the following equation:

$$K_d = \frac{\text{amount of metal ion in the exchanger phase/g of exchanger}}{\text{amount of metal ion in the solution phase/ml of solution}} \quad (1)$$

3. Results and discussion

3.1. Synthesis and characterization

Conditions for the synthesis of NATP-*n* are listed in Table 1. The formation of NATP-*n* crystals was observed to be sensitive to the pH and Ti/Al molar ratio of the initial mixture. When $8 \leq pH \leq 9$ and $0 \leq Ti/Al \leq 1$, pure samples with the crystal structure of NATP could be obtained. Some crystal impurities appeared in the resulting samples when $9 < pH < 10$, $7 < pH < 8$ or $Ti/Al > 1$, and at a certain pH, the purity of samples decreased and the size of crystals increased with the increase of Ti/Al. NATP-*n* could not be obtained when $pH > 10$ or $pH < 7$. Fig. 1 shows the powder XRD patterns of NATP-*n* samples (pH 8.5 in the initial mixture). It is found that NATP-0.5 has the highest relative crystallinity comparing the intensity of diffraction peaks. The SEM photo of NATP-0.5 (Fig. 2) reveals that the crystals are homogeneous with hexagonal prisms. The crannies on crystal surface were resulted from high electron beam bombardment. The crystal structure according to single-crystal XRD data has been described detailly in our previous paper: a negatively charged 2D layered framework is constitutive of PO_4 tetrahedral units linked by corners to MO_4F_2 (M = Al, Ti) octahedral units, Na^+ cations locating in the interlamellar space and the cavities of framework (Fig. 3).

The results of chemical stability detection show that NATP-0.5 can exist stably in 10^{-3} M acid and 1 M alkali solutions. After impregnation in acid and alkali solutions for 24 h, the relative crystallinity of samples decreased to 95.5% (1 M sodium hydroxide), 87.8% (10^{-3} M nitric acid) and 47.5% (1 M nitric acid), respectively.

3.2. Ion-exchange equilibrium

Table 2 shows the ion-exchange capacities and the distribution coefficients for H^+ and some metal ions by employing NATP-0.5 as a cation exchanger. The maximum ion-exchange capacity is found to be 12.74 mequiv./g for H^+ ions. High exchange capacities for Li^+ and Pb^{2+} (6.98 and 3.92 mequiv./g, respectively) are observed. These values are higher than those reported in the literatures, which makes NATP-*n* a promising cation exchangers. The affinity sequence for the mono- and divalent metal ions is $Li^+ > Pb^{2+} > Ni^{2+} > Zn^{2+} > Mg^{2+} > Co^{2+} \sim Mn^{2+} > Ba^{2+} > Ca^{2+}$. The order is not

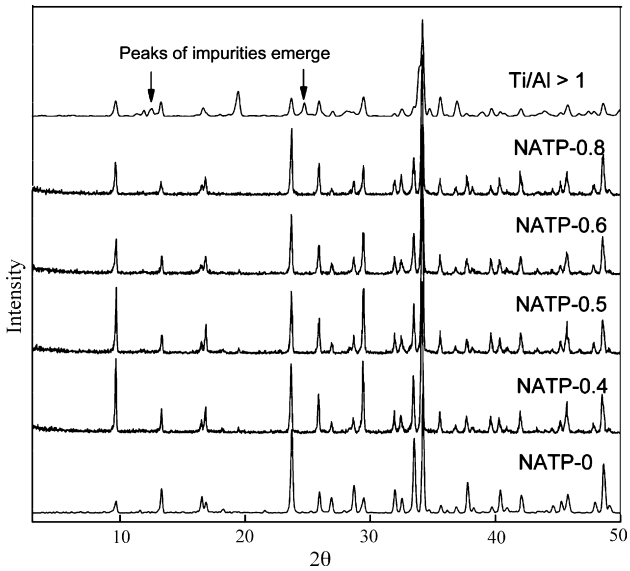

Fig. 1. XRD of NATP-*n* samples.

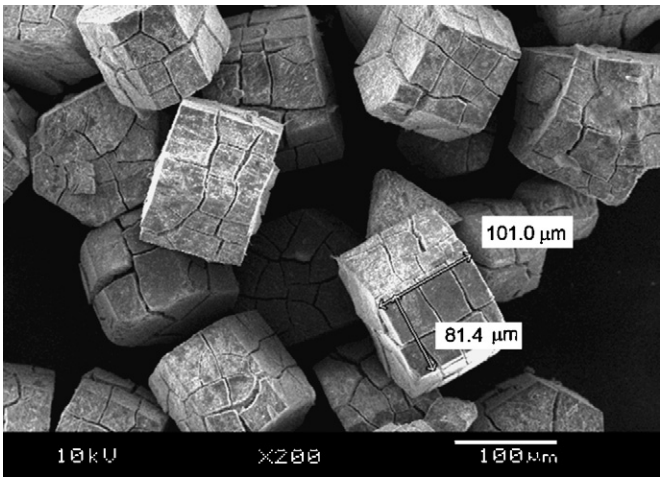

Fig. 2. SEM photo of NATP-0.5.

in agreement with the size of metal ions, suggesting the existence of other influential factors. XRD analyses revealed that samples after the ion exchange kept the crystal structure. Therefore, the whole ion exchange process can be represented simply as Fig. 4. The use of this model to study the adsorption in solution is based on the results reported by Valenzuela-Calahorro and coworkers [18]. Desolations of hydrated metal ions must occur before the metal ions entering into NATP-0.5, considering the short interlamellar distance in crystal framework.

Considering the relationship equation between standard Gibbs energy of reaction $\Delta_r G$ and Gibbs free energy of formation $\Delta_f G$, $\Delta_r G$ can be expressed as follows:

$$\Delta_r G = \sum_B v_B \Delta_f G(B) \tag{2}$$

To simplify the discussion, we just consider the standard state because the influence of ion properties on Gibbs energy and standard Gibbs energy is consistant according to Gibbs–Duhem equation. The standard Gibbs energy of exchange reaction is

$$\Delta_r G_m^\theta = \Delta_r G_{m1}^\theta + \Delta_r G_{m2}^\theta = Z_A \Delta_f G_{Na-H_2O}^\theta + (m-n)\Delta_f G_{H_2O}^\theta + \Delta_f G_{A-NATP}^\theta - \Delta_f G_{NATP-Na}^\theta - \Delta_f G_{A-H_2O}^\theta \tag{3}$$

where n is 5.2, $\Delta_f G_{H_2O}^\theta$ and $\Delta_f G_{Na^+}^\theta$ are -237.19 and -261.88 kJ mol^{-1}, respectively.

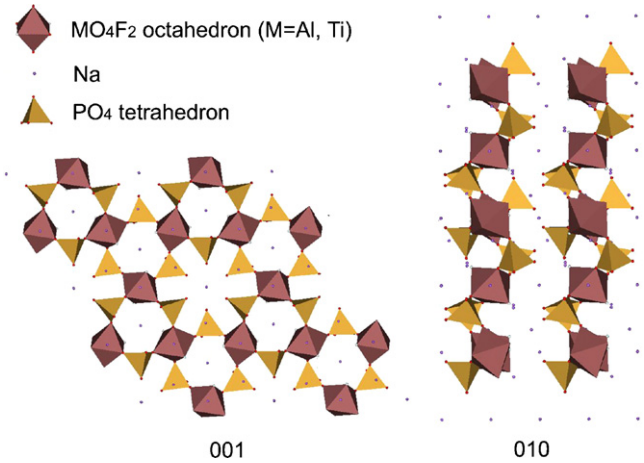

Fig. 3. Polyhedral representation of the structure of NATP [12].

Table 2
Exchange capacities and distribution coefficients for various ions

Ions	Ionic radii (Å)	$\Delta_f G_m^\theta$ (kJ mol^{-1})	Exchange capacities (mequiv./g)	K_d (ml/g)
H^+	0.012	0	12.74	259.8
Li^+	0.760	−293.8	6.98	40.6
Ni^{2+}	0.710	−48.2	0.89	4.5
Mg^{2+}	0.720	−456.0	0.16	0.8
Zn^{2+}	0.740	−147.2	0.40	2.0
Co^{2+}	0.745	−51.5	0.24	1.2
Mn^{2+}	0.750	−223.4	0.13	0.7
Ca^{2+}	0.990	−553.1	0.02	0.1
Pb^{2+}	1.190	−24.3	3.92	64.5
Ba^{2+}	1.350	−560.7	0.02	21.3

Basing the definition on the standard Gibbs free energy of formation, $\Delta_f G^\theta_{A-OH_2}$ can be expressed as

$$\Delta_f G^\theta_{A-OH_2} = \Delta_f G^\theta_{A^{Z+}} - \Delta_f G_{sol} \tag{4}$$

where $\Delta_f G_{sol}$ is the Gibbs free energies of solvation, according to Born theory, whose calculation formula is

$$\Delta_f G_{Sol} = -\frac{L(Z_A e)^2}{8\pi\varepsilon_0 r_A}\left(1 - \frac{1}{\varepsilon_r^*}\right) \tag{5}$$

where r_A is the ionic radii, Z_A is ionic charge, L is Avogadro's constant, ε_0 is dielectric constant in vacuum, ε_r^* is the relative dielectric constant of water.

So Eq. (6) is obtained by subtracting Eq. (4) from (3):

$$\begin{aligned}
\Delta_r G^\theta_m &= Z_A\Delta_f G^\theta_{Na-H_2O} + (m-n)\Delta_f G^\theta_{H_2O} + \Delta_f G^\theta_{A-NATP} - \Delta_f G^\theta_{NATP-Na} - \Delta_f G^\theta_{A-H_2O} \\
&= Z_A\Delta_f G^\theta_{Na-H_2O} + (m-n)\Delta_f G^\theta_{H_2O} + \Delta_f G^\theta_{A-NATP} - \Delta_f G^\theta_{NATP-Na} - \Delta_f G^\theta_{A^{Z+}} + \Delta_f G_{sol} \\
&= \Delta_f G^\theta_{A-NATP} + \Delta_f G_{sol} + 237.19(n-m) - \Delta_f G^\theta_{A^{Z+}} - (\Delta_f G^\theta_{NATP-Na} + 261.88Z_A) \\
&= \Delta_f G^\theta_{A-NATP} + \Delta_f G_{sol} - \Delta_f G^\theta_{A^{Z+}} + (-237.19m - 261.88Z_A) - \Delta_f G^\theta_{NATP-Na} + 237.19n
\end{aligned} \tag{6}$$

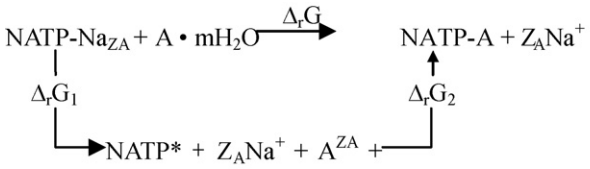

NATP: Solid ion exchanger.
Na^+: Exchanged ion (initially bound to exchange sites of NATP)
m: Hydration number of A.
n: Hydration number of Na^+.
A: Ion initially present in solution.
$\Delta_r G$: Free energy of the overall ion-exchange
$\Delta_r G_1$: Free energy of dissociation of NATP−Na$_{(ZA)}$ and A•mH$_2$O
$\Delta_r G_2$: Free energy of formation of NATP−A and Na^+• nH$_2$O
Z_A: Charge of ion A, 1 or 2.

Fig. 4. Exchange process of NATP for ions in solution.

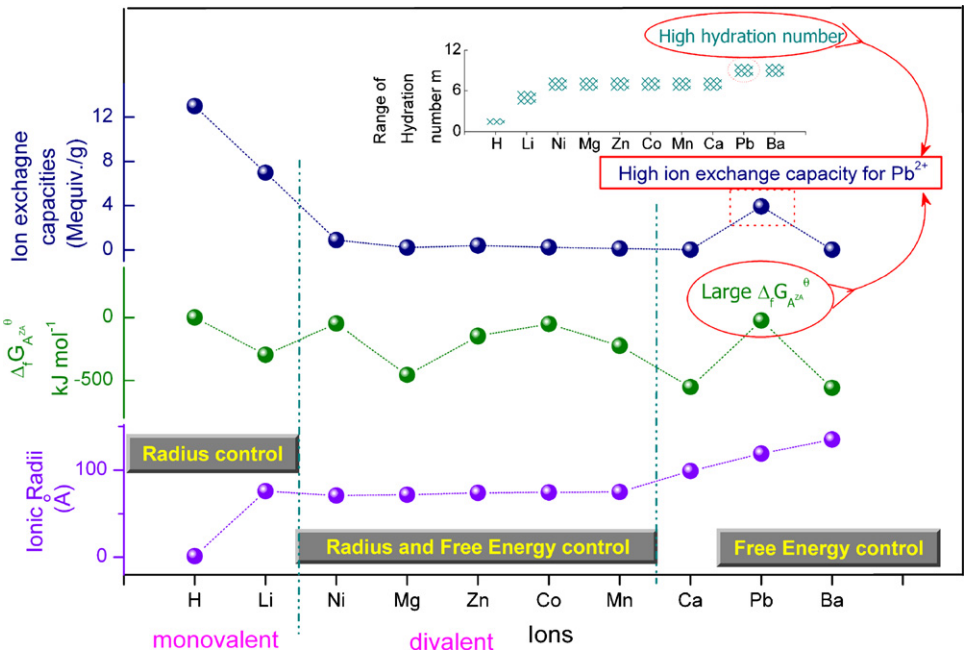

Fig. 5. Influence of ionic radii, hydration numbers and standard Gibbs free energies on exchange capacities.

So $\Delta_f G^{\theta}_{A-NATP}$, $\Delta_f G_{sol}$, hydration number m, Z_A and $\Delta_f G^{\theta}_{A^{Z+}}$ are the decisive factors of the ion-exchange capacity on NATP.

Since the negatively charged 2D layered framework of NATP-*n* has high stability and the Na^+ cations locating in the interlamellar space and the cavities of framework (six different crystal sites in total) have high mobility, the ion exchange in NATP-*n* is that A^{Z+} ions enter these crystal sites replacing Na^+ cations, which does not affect the crystal framework nearly. Therefore, to different metal ions, the difference of the value of $\Delta_f G^{\theta}_{A-NATP}$ is mainly decided by the characters of A^{Z+} ions themselves. If A^{Z+} ions with smaller radii and similar ionic structure to Na^+ enter NATP*, the crystal structure of A–NATP is more stable, resulting in smaller $\Delta_f G^{\theta}_{A-NATP}$. According to Eq. (5), $\Delta_f G_{sol}$ increases with the decrease of charge and increase of radii. Basing the research of Rasaiah and Lynden, the hydration number m increases with the increase of r_A [19] and $(-237.19m–261.88Z_A)$ decreases with the increase of r_A and Z_A.

Fig. 5 shows the relationships of exchange capacities with ionic radii r_A, hydration number m and standard Gibbs free energy $\Delta_f G^{\theta}_{A^{Z+}}$. H^+ has the highest ion exchange capacity because of its rather small ionic radii and large $\Delta_f G^{\theta}_{H^+}$. For alkali metal ions, the difference of their hydration numbers and $\Delta_f G^{\theta}_{A^{Z+}}$ ($\Delta_f G^{\theta}_{Li^+}$, $\Delta_f G^{\theta}_{Na^+}$, and $\Delta_f G^{\theta}_{K^+}$ are -293.80, -261.88 and -282.25 kJ mol^{-1}, respectively) are not very big, so their exchange capacities are decided mainly by ionic radii, which is the reason why ion-exchange capacities change with ionic radii. For divalent metal ions, they are divided into two types according the ionic radii. (1) The ions with the radii between 0.71 and 0.75 Å include Ni^{2+}, Mg^{2+}, Zn^{2+}, Co^{2+} and Mn^{2+}. Their hydration numbers are in the range of 6–8. Among these ions, Ni^{2+} has the highest ion-exchange capacity because of its small radii and high $\Delta_f G^{\theta}_{Ni^{2+}}$. For the ions in this range, there is not big value difference between $|\Delta_f G^{\theta}_{A-NATP} + \Delta_f G_{sol}|$ and $|\Delta_f G^{\theta}_{A^{Z+}}|$ and their exchange capacities are decided by ionic radii and the standard Gibbs free energy of formation: the ion with smaller radii and higher Gibbs free energy of formation has higher ion-exchange capacity. (2) The ions with larger radii include Ca^{2+}, Pb^{2+} and Ba^{2+}. Their hydration numbers are in the range of 6–8 for Ca^{2+} and 8–10 for Pb^{2+} and Ba^{2+}. Their $\Delta_f G^{\theta}_{A-NATP}$ and $\Delta_f G_{sol}$ are bigger than (1) due to their larger ionic radii, while $\Delta_f G^{\theta}_{A-NATP}$ and $\Delta_f G_{sol}$ are negative leading to $|\Delta_f G^{\theta}_{M-NATP\text{-}n} + \Delta_f G_{sol}|$ small. For the ions in this range, $|\Delta_f G^{\theta}_{A-NATP} + \Delta_f G_{sol}| << |\Delta_f G^{\theta}_{M^{Z+}}|$, so their exchange capacities are decided by the standard Gibbs free energy of formation. The large $\Delta_f G^{\theta}_{A^{Z+}}$ and hydration number are the reasons why the Pb^{2+} exchange capacity is higher even than other divalent metal ions with smaller radii.

Table 3
Distribution coefficients for Li^+ and Pb^{2+} in the synthetic mixtures

Ions	K_d (ml/g)
Mixed solution I	
Li^+	231.1
K^+	9.8
Sr^{2+}	1.6
Mg^{2+}	4.2
Ca^{2+}	0.2
Ba^{2+}	0.2
Mixed solution II	
Pb^{2+}	23.3
Ni^{2+}	0.06
Mg^{2+}	–
Co^{2+}	–
Ca^{2+}	3.2
Zn^{2+}	0.03
Ba^{2+}	10.8

3.3. Selective extraction for Li^+ and Pb^{2+}

Table 3 shows the results of selective extractions for Li^+ from the synthetic mixture I containing Li^+, Sr^+, K^+, Mg^{2+}, Ca^{2+} and Ba^{2+}, and for Pb^{2+} from the synthetic mixture II containing Pb^{2+}, Ca^{2+}, Ba^{2+}, Co^{2+}, Ni^{2+}, Zn^{2+} and Mg^{2+} on NATP-0.5. The distribution coefficients for Li^+ and Pb^{2+} are much higher than other ions, indicating that NATP is a promising selective inorganic ion exchanger for Li^+ and Pb^{2+} ions.

4. Conclusions

NATP-n is a novel inorganic ion exchanger with high chemical and thermal stability. The promising feature is the exchange selectivity for Li^+ and Pb^{2+} ions. Its exchange capacities for H^+, Li^+ and Pb^{2+} are obviously higher than most inorganic ion exchangers and ion exchange resins, due to a large number of Na^+ cations with high mobility in the interlamellar space and the cavities of the framework. This material can be used for the ion-selective electrode for the selective determination of microquantities of Pb^{2+} in solutions and ion sieve to extract lithium in the nature.

References

[1] C.B. Amphlet, Inorganic Ion Exchangers, Elsevier, Amsterdam, 1964.
[2] A. Clearfield, G.H. Nancollas, R.H. Blessing, Ion Exch. Solvent Extr. 5 (1973) 3.
[3] R. Niwas, A.A. Khan, K.G. Varshney, Colloids Surf. A 150 (1999) 7.
[4] K.G. Varshney, N. Tayal, A.A. Khan, R. Niwas, Colloids Surf. A 181 (2001) 123.
[5] A.M.A. Ibrahim, Polyhedron 18 (1999) 2711.
[6] M.E. Malla, M.B. Alvarez, D.A. Batistoni, Talanta 57 (2002) 277.
[7] M.E. Meima, J.R. Mackley, D.L. Barber, Curr. Opin. Nephrol. Hypertens. 16 (2007) 365.
[8] M.A. Keane, Colloids Surf. A 138 (1998) 11.
[9] A.A. Khan, M.M. Alam, React. Funct. Polym. 55 (2006) 277.
[10] Z.M. Siddiqi, D. Pathania, J. Chromatogr. A 987 (2003) 147.
[11] Y. Zhang, P. Tian, Z.G. Sun, Z.Y. Liu, Y.Y. Zhang, L.H. Qu, S.Y. Sang, Z.M. Liu, Solid State Commun. 141 (2007) 407.
[12] A.G. Kholmogorov, O.N. Kononova, O.N. Panchenko, Can. Metall. Quart. 43 (3) (2004) 297–303.
[13] G. Gelbard, Ind. Eng. Chem. Res. 44 (2005) 8468.
[14] T.W. Xu, J. Membr. Sci. 263 (2005) 1.
[15] A. Mushtaq, J. Radioanal. Nucl. Chem. 262 (2004) 797.
[16] V. Anand, R. Kandarapu, S. Garg, Drug Discov. Today 6 (2001) 905.
[17] A. Hedstrom, J. Environ. Eng. 127 (2001) 673.
[18] A.N. Guijosa, R.N. Casas, C.V. Calahorro, J.D.L. González, A.G. Rodríguez, J. Colloid Interface Sci. 264 (2003) 60.
[19] J.C. Rasaiah, R.M. Lynden-Bell, Computer simulation studies of the structure of ions and non-polar solute in water, Philos. Trans. R. Soc. Lond. (2001) 359.